



# Observation of a common symmetry for the pseudogap and the superconducting order parameter near the surface of underdoped $\text{YBa}_2\text{Cu}_3\text{O}_{6+x}$

G. Koren<sup>\*</sup>, L. Shkedy, E. Polturak

*Physics Department, Technion, Israel Institute of Technology, Haifa 32000, Israel*

Received 27 August 2003; received in revised form 11 November 2003; accepted 17 November 2003

## Abstract

Measurements of the angular dependence of conductance spectra in the  $a$ - $b$  plane of underdoped  $\text{YBa}_2\text{Cu}_3\text{O}_{6+x}$  junctions are reported. At zero magnetic field the superconducting gap shows a  $|d + is|$ -like symmetry. Application of a magnetic field strongly suppresses this gap leaving only the pseudogap feature which also shows a  $|d + is|$ -like angular dependence. We thus observe the same symmetry for the superconducting gap and the pseudogap characterizing the YBCO electrodes near the interface with the barrier. An  $H_{c2}$  value of  $\sim 5$  T of the secondary (is) order parameter can also be deduced from our results.

© 2003 Elsevier B.V. All rights reserved.

*PACS:* 74.20.Rp; 74.50.+r; 74.72.Bk

*Keywords:* Pseudogap; d-wave superconductor; Energy gap; Weak links

## 1. Introduction

The concept of the pseudogap in the context of high temperature superconductivity was first suggested by Alloul et al. who measured nuclear magnetic resonance (NMR) of Y in  $\text{YBa}_2\text{Cu}_3\text{O}_{6+x}$  (YBCO) [1]. Later, the presence of the pseudogap was demonstrated by many different techniques, for example in measurements of angular resolved photo-emission (ARPES) [2], transport studies [3], tunneling measurements [4], and conductance

spectroscopy in junctions [5]. A comprehensive review of experimental studies of the pseudogap in the HTS materials was given by Timusk and Statt [6]. In particular, Deutscher had shown the existence of two distinct energy scales (energy gaps) in the high temperature superconductors (HTS) [5]. One is the ordinary superconducting gap  $\Delta$  which exists at  $T \leq T_c$ , while the other is the pseudogap which opens up at  $T^*$  or  $T_p$ , both above  $T_c$ . Recently, a pseudogap signature was observed also in the electron doped HTS [7]. The origin of the pseudogap is a subject of intensive studies. Several authors suggested that this regime is characterized by the presence of pre-formed Cooper pairs, which however do not exhibit long range phase coherence [8]. Alternate models suggest that

<sup>\*</sup> Corresponding author.

*E-mail address:* [gkoren@physics.technion.ac.il](mailto:gkoren@physics.technion.ac.il) (G. Koren).

*URL:* <http://physics.technion.ac.il/~gkoren> (G. Koren).

the pseudogap region results from strong superconducting fluctuations [9], antiferromagnetic correlations [10], or separation of spin and charge [11]. Currently, there is not enough experimental information to decide which of these models presents the correct description of the origin of the pseudogap. For example, one could interpret the microwave spectroscopy experiments of Corson et al. [12], and the Nernst effect measurements by Xu et al. [13], as supportive of the pre-formed pairs scenario. On the other hand, the null results of experiments searching for Andreev reflections above  $T_c$  is pointing against it [14,15]. It is the aim of the present paper to add experimental information which could be useful to discriminate between the various models. In our previous studies we used underdoped YBCO based ramp type (or edge) junctions, to measure the full angular dependence of the conductance spectra in the  $a$ – $b$  plane. We found that the superconducting order parameter shows a modified  $d_{x^2-y^2}$  wave behavior with an extended node region and a non-zero gap at the node [16]. We also investigated the temperature and magnetic field dependence of the conductance spectra and found three distinct energy scales, which could be distinguished under different fields and temperatures. These were attributed to the two superconducting  $d_{x^2-y^2}$  and  $is$  (or  $id_{xy}$ ) energy gaps, and the pseudogap [17]. In the present work we extend our study to determine the angular dependence of the pseudogap. We find the same angular dependence for the superconducting gap and the pseudogap near the surface of underdoped YBCO as was already found before in BSCO [2], and discuss some possible reasons of this behavior.

## 2. Experimental

Our underdoped YBCO based ramp type junctions with  $\text{YBa}_2\text{Fe}_{0.45}\text{Cu}_{2.55}\text{O}_{6+x}$  barrier were described before [16–18]. Briefly, they consist of all epitaxial thin film layers of  $c$ -axis orientation with electrodes which are coupled through the junction in the  $a$ – $b$  plane. The films were prepared by laser ablation deposition, and patterning was done by deep UV photo-lithography and Ar ion milling. The junctions were found to have an extremely

smooth interface of less than a nanometer roughness [16]. The multilayer thin film structure was patterned into 10 junctions on the (100)  $\text{SrTiO}_3$  wafer, each in a different direction ( $\theta$ ) in the  $a$ – $b$  plane of the films. By the use of three separate milling steps of the base electrode, similar ramp angles of  $\sim 35 \pm 5^\circ$  were obtained for all 10 junctions on the wafer. Typical film thicknesses are 90 nm for the base and cover electrodes and 22 nm for the barrier, while the width of each junction is 5  $\mu\text{m}$ . A gold layer is deposited on top of the whole wafer and patterned to produce the  $10 \times 4$  contact pads for the 4-terminal transport measurements.

## 3. Results and discussion

Fig. 1 shows the resistance versus temperature of 6 of the 10 junctions on a wafer. Compared to our previous study [16], less oxygen was used in the annealing process resulting in much more resistive junctions ( $\times 5$ ) and underdoped YBCO electrodes which become superconducting at  $\sim 50$  K as compared to 60 K used previously [16,18]. The normal state resistance is typical of underdoped  $\text{YBa}_2\text{Cu}_3\text{O}_y$ , with  $6.50 \lesssim y \lesssim 6.55$  [19]. For junctions with orientation close to the  $a$  or  $b$  axes, the resistance goes through a minimum at 40 K, in-

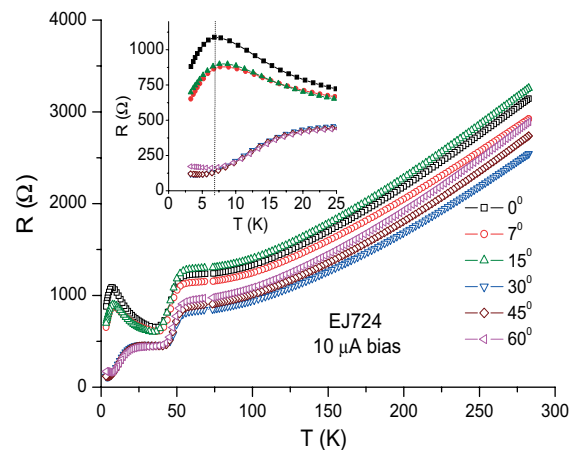


Fig. 1. Resistance versus temperature of six of the ten junctions on the wafer. The inset shows the low temperature region, illuminating the difference between junctions along the main axes (solid symbols) and near the node (open symbols).

creases to a local maximum at 7 K and then decreases at lower temperature. For junctions with orientation near the node, the normal resistance  $R_N$  stays almost constant between 40 and 20 K and then decreases with temperature down to 7 K, where it starts increasing again slightly. Similar to our previous results [16], we find that the  $R_N$  values of the  $30^\circ$ ,  $45^\circ$  and  $60^\circ$  junctions are the lowest. This result is consistent with the  $d_{x^2-y^2}$ -wave anisotropy of the order parameter where states in the gap near the node region contribute to increase the conductance at low bias.

Fig. 2 shows the normalized conductance measured on four of the ten junctions on the wafer at 3.8 K, and also at 6.4 K for the  $45^\circ$  (node) junction. The absolute values of the conductance at zero bias can be inferred from the resistance values in Fig. 1 which were measured at low bias. Like in our previous studies [16,17], we find a different bias dependence of the conductance spectra for junctions near the node orientation ( $30^\circ$ ,  $45^\circ$  and  $60^\circ$ ) and the one near the main axis ( $0^\circ$  and  $15^\circ$ ). For the sake of simplicity, we take the measured energy gap  $\Delta$  of our junctions as the peak to peak voltage difference divided by 4. The resulting  $\Delta(\theta)$  is shown in the inset of Fig. 2 together with the gap

values measured in our previous study [16] and the expected form  $\Delta_0|\cos(2\theta)|$  where  $\Delta_0 = 20$  mV. Both sets of data agree quite well, and the dominant  $d_{x^2-y^2}$ -wave symmetry is clearly seen. We single out the spectra of the  $\theta = 45^\circ$  junction, which exhibits a zero bias conductance peak at 6.4 K, consistent with a  $d_{x^2-y^2}$ -wave order parameter. At a lower temperature, this peak splits, implying the emergence of a secondary order parameter, previously observed by others [20,21]. The finite gap value at  $\theta = 45^\circ$  in our previous work is well reproduced [16,17], and equals  $3 \pm 0.5$  mV, consistent with  $2.5 \pm 0.3$  mV value found before. There is therefore evidence from several sources regarding the existence of an additional sub-dominant component in the pair potential of YBCO near a surface (in our case, the interface with the barrier). Since the gap feature at low bias disappears already at 6.4 K, and a zero bias peak appears as seen in Fig. 2 and also in Ref. [17], it cannot result from a finite tunneling cone which should be independent of temperature. Therefore, the observation can be explained as due to a presence of  $is$  or  $id_{xy}$  components in the order parameter near a surface. To further check this conclusion we also simulated the conductance curve of the  $45^\circ$  junction at 3.8 K using a  $d_{x^2-y^2} + is$  wave order parameter and a model given by Tanaka et al. [22]. The simulation result fits the data very well, and is shown by the solid line in Fig. 2. Attempts to fit the data using a  $d_{x^2-y^2} + s$  wave order parameter were not successful. Another feature seen in the normalized conductance of the node junction in Fig. 2 is that the maximum conductance at low bias is larger than the Andreev limit of 2 for high transparency (low  $Z$ ) junctions. The reason for this is the existence of bound states also at voltage values higher than zero bias [22].

Fig. 3 shows the low temperature conductance spectra of the  $0^\circ$  junction at several magnetic fields normal to the wafer, together with the corresponding gap values versus field. First we note that the maxima of the conductance seen in this figure show a much smaller variation with the field compared to the  $45^\circ$  junction in Fig. 2 (17% versus 250%). The inset of Fig. 3 shows the gap apparently increasing with field. We attribute this apparent behavior to changes in the relative

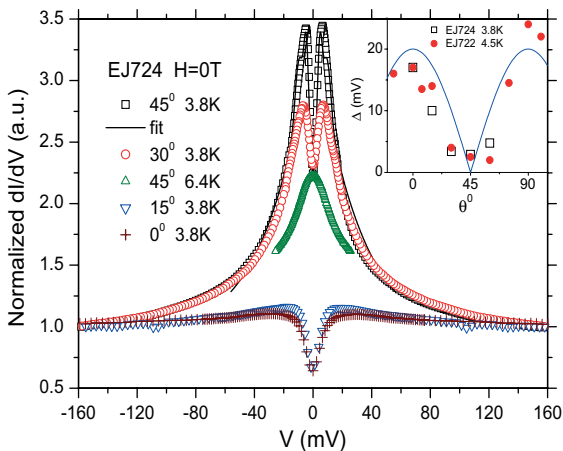


Fig. 2. Normalized conductance versus voltage bias of four of the junctions (the  $60^\circ$  data is omitted for clarity), together with a simulation of the node junction data at 3.8 K (line). The inset shows the angular dependence of the corresponding gaps at 3.8 K (open squares), together with previous gap values taken from Ref. [16] at 4.5 K (solid circles), and  $20|\cos(2\theta)|$  (line).

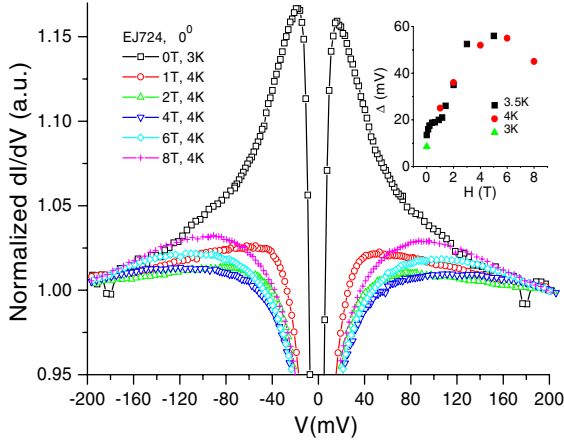


Fig. 3. Conductance spectra at low temperatures of the  $0^\circ$  junction for several magnetic field values (main panel), and the corresponding gap energies versus field (circles and a triangle) together with more data (squares) from Ref. [17] (inset).

spectral weight of the superconducting gap and the pseudogap induced by the magnetic field. With the application of a magnetic field, first the strongest feature attributed to the  $is$  or  $id_{xy}$  component of the order parameter is suppressed, followed by the  $d_{x^2-y^2}$  component, finally leaving only the pseudogap feature which appears at the highest energy. Similar observations were reported by Krasnov et al. in intrinsic BSCO junctions [24]. Their conductance spectra have also shown suppression of characteristic features with increasing field, while the apparent gap energies were observed to either decrease or increase with field depending on temperature. Above  $T_c$  in our junctions, the leads to the junction become normal and their resistance becomes much larger than that of the junction. Hence, measurements of the conductance spectra above  $T_c$  are not possible. We therefore used the magnetic field to suppress superconductivity at low temperature, as was done recently also by Alff et al. [7]. In our previous observations, the apparent peak position of the conductance in the  $0^\circ$  junction was found to decrease with increasing field up to 5 T [16]. The reason for the difference from the present results can be due to the fact that the present junctions are much more resistive and thus more in the tunneling-like regime. The inset of Fig. 3 shows that upon increasing the field up to

1.1 T, the position of the peak in the conductance spectra increases from 9 to 20 mV with a plateau at  $\sim 19$  mV which is similar to the  $d$ -gap value of the 60 K YBCO phase measured previously ( $16 \pm 1.5$  mV) [23]. This effect is attributed to the suppression of the  $is$  component whose signature disappears already at  $\sim 0.2$  T. At higher fields, the  $d_{x^2-y^2}$  gap signature in the conductance is also suppressed (at  $\sim 1.4$  T), and the conductance spectra exhibit only a peak around 110 mV which corresponds to a gap value of 55 mV. This value is characteristic of the pseudogap in underdoped YBCO, and we therefore identify this feature as the pseudogap [25]. At 8 T, the peak position again decreases slightly.

Why should a field in the range of a few Tesla (small compared to  $H_{c2}$ ) suppress the  $d_{x^2-y^2}$  gap signature (of the 50 K YBCO phase) at 4 K is puzzling, but the large 50–60 mV gap values observed here are clearly due to the pseudogap and not the  $d_{x^2-y^2}$  gap [25]. We suggest the possibility that superconductivity near the interface is weakened by the proximity effect with the normal barrier. This effect is apparently much stronger in our new, more resistive junctions. Preliminary results using junctions with a *non-magnetic* Ga doped YBCO barrier, also show similar behavior in magnetic fields as observed in the present study in junctions with a Fe doped YBCO barrier. It is therefore quite unlikely that the depression results from scattering in the barrier, as the result seems independent of the type of dopant used in the tunneling barrier. We also note that conductance spectra in which the relative spectral weight of the pseudogap feature is larger than the  $d$ -gap were observed before, even at zero field [5,25]. Thus the  $d_{x^2-y^2}$ -wave characteristic is not fully suppressed at 1–2 T, but only becomes weaker in comparison with the pseudogap. Recently, an  $H_{c2}$  value of about 35 T was measured for underdoped YBCO with  $T_c = 50$  K like we use here [19]. This relatively low  $H_{c2}$  value together with a weaker superconductivity near the interface, can also help explain the surprisingly strong suppression of the  $d$ -wave characteristic. Going back now to the results in the inset of Fig. 3, one can deduce that the ratio of critical fields  $H_{c2}(d_{x^2-y^2})/H_{c2}(is)$  in underdoped YBCO is of the order of  $1.4/0.2 = 7$ . Taking

$H_{c2}(d_{x^2-y^2})$  as 35 T, we can estimate that the critical field of the *is* component of the order parameter should be of about 5 T.

Fig. 4 shows the conductance spectra of the 45° junction at 4 K under several magnetic fields normal to the wafer, together with the corresponding gap values. As discussed before, since a pure  $d_{x^2-y^2}$ -wave order parameter has no gap along the node, the prominent features at small fields in the conductance characteristics of Fig. 4 must be due to the small *is*-wave component [16,17]. We find that with increasing field, the whole conductance spectrum is almost totally suppressed, similarly to what was observed with the 0° junction. We attribute the non-conservation of spectral weight in the normalized conductance spectra versus field to the breaking of bound states which are prevalent at energies  $E \lesssim 2\Delta_d$  [22]. The position of the conductance peak increases significantly, from 3 mV at 0 T to 7.5 mV at 8 T as seen in the inset of this figure. As was explained above, the larger gap values seen at high fields (see inset of Fig. 3) are due to the pseudogap. Therefore, the conductance characteristics at high fields in Fig. 4 must also be due to the pseudogap. It seems that by applying an 8 T field, we can apparently “erase” all other features except the pseudogap. We are therefore in the position to perform a clean

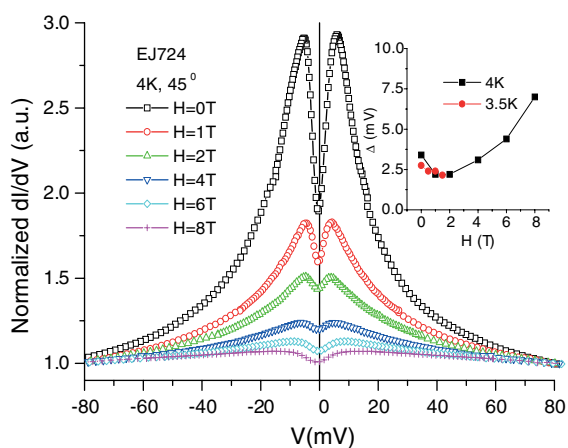


Fig. 4. Conductance spectra at 4 K of the 45° junction at several magnetic fields (main panel), and the field dependence of the corresponding gap energies together with more data at 3.5 K (inset).

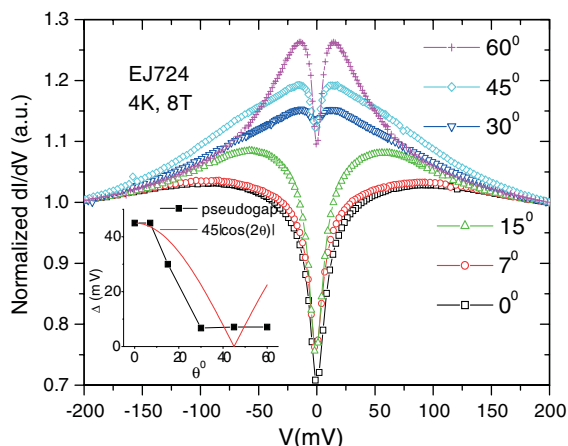


Fig. 5. Normalized conductance spectra at 4 K and 8 T of six junctions (main panel), and the angular dependence of the pseudogap and  $45|\cos(2\theta)|$  (inset).

measurement of the angular dependence of the pseudogap in underdoped YBCO.

Fig. 5 presents the main message of this study. It shows the normalized conductance spectra at 4 K and 8 T of six junctions with different orientations in the *a*-*b* plane (main panel), and the resulting angular dependence of the measured pseudogap feature (inset). We find that the angular dependence of the pseudogap is the same as that of the superconducting gap given in the inset of Fig. 2 (to within experimental error). This indicates that the two phenomena might have a common origin. The most obvious reason is that both are related to the intrinsic crystalline symmetry of YBCO. It would appear that since the signature of the superconducting gap disappears with the application of a magnetic field and that of the pseudogap does not, the pseudogap is not connected with superconductivity. However, since the value of the magnetic field needed to suppress these features seems to depend on the energy of the peak in the conductance curve, it could be that the field we have at our disposal (8 T) is simply insufficient for the suppression of the pseudogap feature. Hence, other scenarios which are consistent with the present results cannot be ruled out. One such scenario is that of the possible existence of uncorrelated pre-formed pairs in the pseudogap regime [26]. These pairs have the same symmetry of the

pair-wave function as that of the correlated pairs and can thus naturally yield the same symmetry for the pseudogap and the superconducting gap.

It should be noted though that angular resolved photo-emission measurements (ARPES) of the angular dependence of the gap and the pseudogap have been done before in BSCO 2212 by Ding et al. [2]. They found that there is basically no significant difference between the observed gap below and above  $T_c$ . The magnitude and angular dependence of the gap and pseudogap was almost the same, except for the observation of a broader node region for the pseudogap. The error in the ARPES measurements however, in the values of the energy gap of the heavily underdoped BSCO was quite large, about  $\pm 60\%$ . In contrast, the error in the present conductance measurements in the determination of the energy gap values near the node region is much smaller, about  $\pm 20\%$ . Therefore, the added value of the present results is the higher energy resolution, the use of a different (tunneling) technique, and the fact that we study another material, underdoped YBCO.

#### 4. Conclusions

In conclusion, our results of the angular dependence of the conductance demonstrate clearly that both the superconducting gap and the pseudogap have the same  $|d_{x^2-y^2} + is|$ -like symmetry in underdoped YBCO near the interface of the junctions. This result, combined with the similar result found for underdoped BSCCO [2], imposes another constraint on the theoretical description of the pseudogap. We also found that  $H_{c2}$  of the small  $c$  component of the order parameter is of the order of 5 T.

#### Acknowledgements

We are grateful to A. Auerbach, O. Millo, G. Deutscher and I. Lubimova for useful discussions. We also thank I. Lubimova for use of her conductance simulation program. This research was supported in part by the Israel Science Foundation, the Heinrich Hertz Minerva Center for HTS,

the Karl Stoll Chair in advanced materials, and by the Fund for the Promotion of Research at the Technion.

#### References

- [1] H. Alloul et al., *Phys. Rev. Lett.* 63 (1989) 1700.
- [2] H. Ding, M.R. Norman, T. Mochiku, K. Kadowaki, J. Giapinzakis, *Nature* 382 (1996) 51.
- [3] J.R. Cooper et al., *J. Phys. I* 6 (1996) 2237.
- [4] Ch. Renner, B. Revaz, J.Y. Genoud, K. Kadowaki, O. Fischer, *Phys. Rev. Lett.* 80 (1998) 149; A.J. Gupta, K.W. Ng, *Phys. Rev. B* 58 (1998) 8901; M. Suzuki, T. Watanabe, *Phys. Rev. Lett.* 85 (2000) 4787.
- [5] G. Deutscher, *Nature* 397 (1999) 410.
- [6] T. Timusk, B. Statt, *Rep. Prog. Phys.* 62 (1999) 61.
- [7] L. Alff, Y. Krockenberger, B. Welter, M. Schonecke, R. Gross, D. Manske, M. Naito, *Nature* 422 (2003) 698.
- [8] V. Emery, S.A. Kivelson, *Nature* 374 (1995) 434.
- [9] A.M. Cucolo, M. Cuoco, A.A. Varlamov, *Phys. Rev. B* 59 (1999) R11675; P. Carretta, A. Lascialfari, A. Rigamonti, A. Rosso, A. Varlamov, *Phys. Rev. B* 61 (2000) 12420; H. Westfahl Jr., D.K. Morr, *Phys. Rev. B* 62 (2000) 5891; I. Ussishkin, S.L. Sondhi, D.A. Huse, *Phys. Rev. Lett.* 89 (2002) 287001.
- [10] A.V. Chubukov, D. Pines, B.P. Stojkovic, *J. Phys.: Cond. Mat.* 8 (1996) 10017.
- [11] (a) G. Kotliar, J. Liu, *Phys. Rev. B* 38 (1988) 5142; (b) P.W. Anderson, *The Theory of Superconductivity in the High  $T_c$  Cuprates*, Princeton University Press, Princeton, NJ, 1997.
- [12] J. Corson, R. Mallozzi, J. Orenstein, J.N. Eckstein, I. Bozovic, *Nature* 398 (1999) 221.
- [13] Z.A. Xu, N.P. Ong, Y. Wang, T. Kakeshita, S. Uchida, *Nature* 406 (2000) 486.
- [14] Y. Dagan, A. Kohen, G. Deutscher, *Phys. Rev. B* 61 (2000) 7012.
- [15] R.S. Gonnelli et al., *Eur. Phys. J. B* 22 (2001) 411, *Cond-mat/0101209*.
- [16] G. Koren, N. Levy, *Europhys. Lett.* 59 (2002) 121, Note that in Fig. 1 of this paper the scales are in nm (Erratum: *ibid* 59 (2002) 634).
- [17] G. Koren, N. Levy, E. Polturak, *J. Low Temp. Phys.* 131 (2003) 849.
- [18] O. Neshet, G. Koren, *Appl. Phys. Lett.* 74 (1999) 3392.
- [19] Y. Ando, K. Segawa, *Phys. Rev. Lett.* 88 (2002) 167005.
- [20] M. Covington, M. Aprili, E. Paraoanu, L.H. Greene, F. Xu, J. Zhu, C.A. Mirkin, *Phys. Rev. Lett.* 79 (1997) 277.
- [21] R. Krupke, G. Deutscher, *Phys. Rev. Lett.* 86 (1999) 4634.
- [22] I. Lubimova and G. Koren, *Phys. Rev. B*, in press, (see *Cond-mat/0306030* (2003)); S. Kashiwaya, Y. Tanaka, *Rep. Prog. Phys.* 63 (2000) 1641; Y. Tanuma, Y. Tanaka, S. Kashiwaya, *Phys. Rev. B* 64 (2001) 214519 (The parameters used in the fit of Fig. 2 are:  $A_d = 16$  mV,  $A_s = 2.6$  mV (at the interface),  $Z = 0.5$  (the

- BTK barrier strength), a tunneling cone of  $\pm 80^\circ$ , and a decay length of  $20\xi_0$ .
- [23] O. Neshet, G. Koren, *Phys. Rev. B* 60 (1999) 9287.
- [24] V.M. Krasnov, A. Yurgens, D. Winkler, P. Delsing, T. Claeson, *Physica C* 352 (2001) 89;
- V.M. Krasnov, A.E. Kovalev, A. Yurgens, D. Winkler, *Phys. Rev. Lett.* 86 (2001) 2657.
- [25] D. Racah, G. Deutscher, *Physica C* 263 (1996) 218.
- [26] M. Buchanan, *Nature* 409 (2001) 8, and references therein.